International Journal of Electrical, Electronic and Communication Sciences
ISSN: 2517-9438
Vol:7, No:2, 2013

Variable Rate Superorthogonal Turbo Code with the OVSF Code Tree

Insah Bhurtah, P. Clarel Catherine, K. M. Sunjiv Soyjaudah

***Abstract*—**When using modern Code Division Multiple Access (CDMA) in mobile communications, the user must be able to vary the transmission rate of users to allocate bandwidth efficiently. In this work, Orthogonal Variable Spreading Factor (OVSF) codes are used with the same principles applied in a low-rate superorthogonal turbo code due to their variable-length properties. The introduced system is the Variable Rate Superorthogonal Turbo Code (VRSTC) where puncturing is not performed on the encoder's final output but rather before selecting the output to achieve higher rates. Due to bandwidth expansion, the codes outperform an ordinary turbo code in the AWGN channel. Simulations results show decreased performance compared to those obtained with the employment of Walsh-Hadamard codes. However, with OVSF codes, the VRSTC system keeps the orthogonality of codewords whilst producing variable rate codes contrary to Walsh-Hadamard codes where puncturing is usually performed on the final output.

***Keywords*—**CDMA, MAP Decoding, OVSF, Superorthogonal Turbo Code.

I. Introduction

THE discovery of turbo codes in 1993 by Berrou, Glavieux and Thitimajshima provided a breakthrough in channel coding such that error-correcting codes with relatively simple structures could permit consistent transmission rates close to the channel capacity with achievable computational complexity. Turbo codes approached the channel capacity by 0.7 dB [1]. In a turbo code system, two or more constituent encoders are involved to different interleaved versions of the same information sequence [2].

Cellular mobile phones are being used every day by millions of people across the world. The number of customers needing services such as short messaging, voice, data, and video is growing. To accommodate the high demand, providers must increase system capacity without degrading the quality of service to an unacceptable level through CDMA. It employs signature codes (rather than time slots or frequency bands) to arrange simultaneous and continuous access to a radio network by multiple users. In other words, it allows many uncoordinated users to transmit simultaneously on the same frequency channel with different spreading codes [3]. A user is given a unique spreading code sequence to spread his data stream before transmission. As all spreading codes are orthogonal to each other, all users can transmit at the same time and channel without any interference. The data of a particular user is recovered by the correlation of received signal with the spreading sequence, and all other interfering signals are rejected as they are orthogonal [3].

In 2009, Ramsawock investigated in a Variable Rate Orthogonal Convolutional (VROC) code which is a variable low rate convolutional code with orthogonal output codewords [3]. This was achieved by the introduction of a puncturing block between the shift register output and the OVSF tree block. The shift register outputs enter a puncturing block which selects the bits to be punctured. Following puncturing, the remaining bits enter the OVSF tree where a codeword is selected. With this method, codewords of variable lengths are obtained [3]. One important aspect of this scheme is that the same trellis is used for decoding. In [4], a Telescopic Protection Code makes use of the variation of the trellis to support the user's input rate variable, instead of puncturing. However, the decoding process is simpler when a fixed trellis is used [3]. The technique in [3] has been attempted in superorthogonal turbo codes. In 1996, Pehkonen and Komulainen designed a superorthogonal turbo code combining principles of low-rate convolutional coding and parallel concatenation using codewords from the Walsh-Hadamard matrix [5]. The same design structure has been used but with OVSF codewords. Iterative decoding is performed with the MAP, log-MAP and max-log-MAP algorithms. The simulation results outperform an ordinary turbo code in [5] but show decreased performance compared to codes employing Walsh-Hadamard codes in [5]. However, the advantage of OVSF codes is that variable-length codes can be obtained in the OVSF tree compared to Walsh-Hadamard codes where a single Walsh-Hadamard matrix of fixed length is used for codeword assignment. The selection of OVSF variable codewords is performed over a single OVSF tree. To achieve the same with Walsh-Hadamard codes, matrices having variable lengths should be stored in memory compared to the storage of a fixed OVSF tree requiring less size. Also, the orthogonality of codewords is kept during puncturing. With Walsh-Hadamard codes, puncturing is often performed on the encoder's final output resulting in destruction of orthogonality of the codewords.

The paper is organized such that in Section II, superorthogonal turbo coding is described and the new code employing OVSF codes is introduced with appropriate descriptions of the encoder and decoder. Section III presents

Insah Bhurtah is an MPhil/PhD student at Electrical and Electronic Engineering Department, University of Mauritius, Mauritius (e-mail: i.bhurtah @ieee.org).

P. Clarel Catherine is a lecturer at Industrial Systems Engineering, School of Innovative Technologies and Engineering (SITE), University of Technology, Mauritius (e-mail: c.catherine@ieee.org).

K.M. Sunjiv Soyjaudah is a professor of Communications Engineering at Electrical and Electronic Engineering Department, University of Mauritius, Mauritius (e-mail: ssoyjaudah@uom.ac.mu).

the variable rate superorthogonal turbo code. In Section IV, simulation results in the AWGN channel are given followed by the conclusion in Section V.

II. Superorthogonal Turbo Coding

Superorthogonal convolutional codes (SCC) are low-rate codes having good distance properties due to bandwidth expansion. Hence, they are used for spread-spectrum applications [6]. The codes are described in [7] and [8]. An SCC is made up of a K_c-2 stage shift register where K_c is the constraint length and K_c-2 stages operate on an orthogonal block encoder consisting of a Walsh-Hadamard orthogonal sequence generator. The K_c-2 stages mean that the first and last stages are excluded and they do not contribute in driving the orthogonal sequence generator. These stages are then modulo-2 added to every bit of the Walsh-Hadamard sequence [3].

The SCC forms the core of the Variable Rate Superorthogonal Convolutional (VRSC) code. Ramsawock showed the VRSC code by introducing a puncturing block [3] as seen in Fig. 1. The block orthogonal encoder was replaced by the OVSF tree so that the code becomes both variable rate and orthogonal [3].

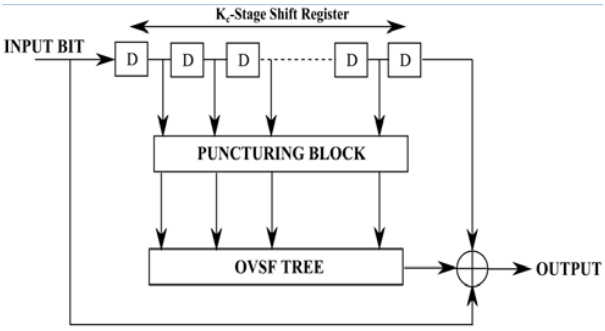

Fig. 1 VRSC Code

The VRSC code has been extended and integrated into a superorthogonal turbo code engaging OVSF codes to provide variable rate and at the same time using the same trellis for decoding all derived rates while maintaining orthogonality between codewords.

A. Motivation for OVSF Code Assignment

Fig. 2 depicts an OVSF code tree where OVSF codes of variable spreading factors (lengths) are obtained. OVSF codes have advantages of accommodating variable-rate services which are important to emerging multimedia applications [9]. This is achieved by the use of variable spreading factors generated from an OVSF code tree. Orthogonal Walsh functions from Hadamard matrices cannot support rate variation due to the fact that the matrices have fixed length. With the OVSF code tree, however, different sequence lengths can be obtained in the same tree. In this work, puncturing was done in the encoder itself to maintain the orthogonality of the OVSF codewords. In CDMA, the loss of orthogonality between spreading codes results in multiple access interference [10]. If Walsh-Hadamard sequences were employed, it would have been impossible to perform puncturing by the deletion of bits from the shift register outputs, as the remaining bits would not have been able to select a different Walsh sequence length in a fixed length matrix. For these codes, puncturing is usually performed by the deletion of bits in the codeword resulting in the destruction of orthogonality.

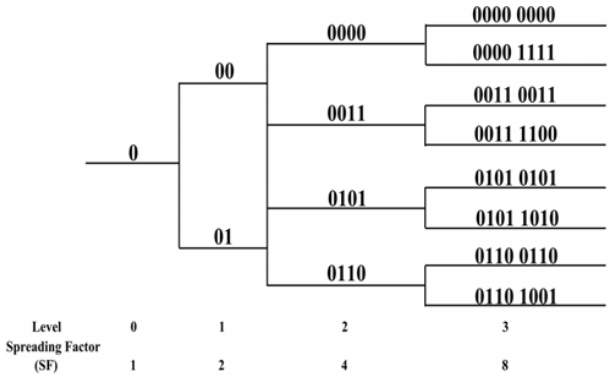

Fig. 2 OVSF Code Tree

In superorthogonal turbo coding, the calculation of the branch metric using MAP algorithm involves a correlation of the received word with the corresponding Walsh or OVSF sequence as will be seen in sub-section II *C*. With puncturing of the codeword at the final output for Walsh-Hadamard codes, a dummy bit is usually inserted during decoding. Hence, during correlation, the value of the branch metric which is fundamental for calculation of alpha and beta and overall decoding, will be different. Variable-rate services are also used in Unequal Error Protection (UEP). The necessity of UEP arises in applications involving speech, audio and video. In CDMA, users need to transmit audio and video where some of the message positions are more sensitive to channel errors while others show less sensitivity [11]. To protect certain parts of the message, the code rate must be varied leading to an important application of codes utilizing OVSF sequences without interference.

B. Encoder

In the recursive superorthogonal turbo encoder, each component consists of a K_c-stage shift register. Fig. 3 shows an encoder having a feedback polynomial 23(octal) with K_c = 5. The original sequence of size N-k (where k is the number of tail bits) is fed to the upper encoder. For each input bit, the inner K-2 stages are excluded (first and last stages) and the remaining bits in the shift registers drive the OVSF code tree to obtain a codeword with length, n = 8. This sequence undergoes a series of module-2 addition operations to give the final codeword. Let the input data sequence be $u = (u^0,u^1,\ldots,u^{(N-k)-1})$. At time t = 0, u^0 produces the output $P_1{}^0 = \{p_1{}^0, p_1{}^1,\ldots,p_1{}^{n-1}\}$ where p is a member of the OVSF sequence.

The way in which the trellis is terminated affects the performance of the code. The procedure in [12] was used, that is by terminating only the upper encoder and leaving the other open. k = 4 tail bits were added to u to drive the encoder state to zero. The output of the upper encoder becomes $P_1=\{P_1^0,P_1^1,\ldots,P_1^{(N-1)}\}$. The original bits u with k tail bits are passed through a pseudorandom interleaver giving u' which enters the lower encoder producing $P_2 = \{P_2^0,P_2^1,\ldots,P_2^{(N-1)}\}$.

Compared to an ordinary turbo code, since the systematic bits are not sent through the channel, there is no common channel output stream for constituent decoders. For each constituent encoder in Fig. 3, the code rate is $^1/_n$, that is $^1/_8$. The overall code rate then becomes $^1/_{16}$.

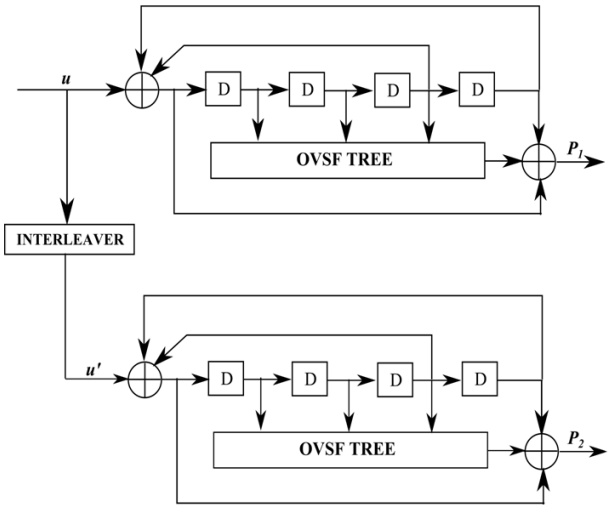

Fig. 3 Superorthogonal Turbo Encoder with the OVSF Code Tree

C. Decoder

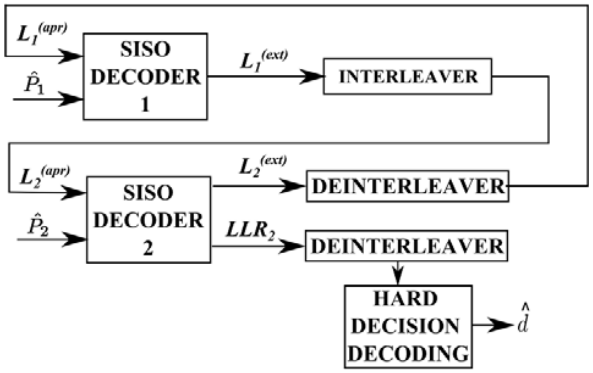

Fig. 4 Superorthogonal Turbo Decoder

The parity bits P_1 and P_2 are multiplexed and modulated using Binary Phase-Shift Keying (BPSK). They are corrupted in an AWGN channel giving $\hat{P}_1$ and $\hat{P}_2$. Decoding of turbo codes is done in an iterative fashion. The decoding algorithm used is the modified BCJR or MAP algorithm [13].

Suppose that the received sequence from an AWGN channel is y, the decoder obtains the sequence which is used by the MAP algorithm to estimate the original transmitted bit sequence u for which the algorithm calculates the a-posteriori log-likelihood ratio LLR, a real number defined by the ratio [2]:

$$LLR = \log \frac{P(u_t = +1|y)}{P(u_t = -1|y)} \quad (1)$$

The numerator and denominator of (1) consist of the a-posteriori conditional probabilities, that is probabilities obtained when y is known. The positive and negative value of LLR shows which bit +1 or -1 was coded at time t.

To calculate the branch metric for any possible state transition, a correlation of the received word and its corresponding OVSF sequence is achieved. The branch probability becomes [6]:

$$\gamma^t = c' \exp\left[U_\xi L^{t(apr)}\right].\exp\left[\sigma^{-2}\sum_i (2p_i^t - 1)\hat{p}_i^t\right] \quad (2)$$

where c' is a constant for all possible parallel transitions, data bits and code symbols, $\xi = (S_t, S_{t-1})$ is any possible state transition of the encoder at time t, $U_\xi \in \{0,1\}$ is the data bit related to ξ, $L^{t(apr)}$ is the a priori estimate given by the previous decoder, σ is the standard deviation of the noise, $t = \{0,1,\ldots,N\text{-}1\}$ and $i = \{0,1,\ldots,n\text{-}1\}$. p_i^t is the symbol of the codeword (OVSF sequence) and $\hat{p}_i^t$ is its corrupted version.

The a-posteriori log-likelihood ratio LLR can also be computed as

$$LLR = \log \frac{\sum_{R_1} \alpha_{t-1}(S_{t-1})\gamma_t(S_{t-1},S_t)\beta_t(S_t)}{\sum_{R_0} \alpha_{t-1}(S_{t-1})\gamma_t(S_{t-1},S_t)\beta_t(S_t)} \quad (3)$$

R_1 and R_0 denote transitions associated with inputs +1 and -1 respectively. The probabilities α and β are calculated recursively by

$$\alpha_t(S_t) = \sum_{S_{t-1}} \alpha_{t-1}(S_{t-1})\gamma_t(S_{t-1},S_t) \quad (4)$$

with initial conditions: $\alpha_0(S_t) = 0$ for $S_t \neq 0$ and $\alpha_0(S_t) = 1$ for $S_t = 0$

$$\beta_{t-1}(S_{t-1}) = \sum_{S_t} \beta_t(S_t)\gamma_t(S_{t-1},S_t) \quad (5)$$

with initial conditions: $\beta_N(S_t) = 0$ for $S_t \neq 0$ and $\beta_N(S_t) = 1$ for $S_t = 0$.

Iterative decoding is achieved as shown in Fig. 4. Two Soft-In Soft-Out (SISO) decoders are used. The output of SISO decoder 1 is expressed as [6]:

$$LLR_1 = L_1^{(apr)} + L_1^{(ext)} \quad (6)$$

where $L_1^{(apr)}$ is the a-priori information provided by the previous decoder. This information is removed from LLR_1 to obtain the extrinsic information, $L_1^{(ext)}$ used as a-priori information by the second decoder.

D. Log-MAP and Max-Log-MAP Algorithms

The MAP algorithm suffers from high complexity, as it needs to perform many multiplications. Simpler versions have evolved such as the log-MAP and the max-log-MAP algorithm which reduce that complexity [14]. Multiplications are replaced by additions. The application of log in (2) yields

$$\Gamma_t = \log\left[c' \exp\left[U_{\xi} L^{t(apr)}\right].\exp\left[\sigma^{-2}\sum_i \left(2p_i^t - 1\right)\hat{p}_i^t\right]\right] \quad (7)$$
$$= c'\left[U_{\xi} L^{t(apr)}\right] + \left[\sigma^{-2}\sum_i \left(2p_i^t - 1\right)\hat{p}_i^t\right]$$

α and β are replaced by A and B. Therefore,

$$A_t(S_t) = \log \alpha_t(S_t) = \max_{S_{t-1}}^{*}\left[A_{t-1}(S_{t-1}) + \Gamma_t(S_{t-1}, S_t)\right] \quad (8)$$

with initial conditions: $A_0(S_t) = 0$ for $S_t = 0$ and $A_0(S_t) = -\infty$ for $S_t \neq 0$

$$B_{t-1}(S_{t-1}) = \log \beta_{t-1}(S_{t-1}) = \max_{S_t}^{*}\left[B_t(S_t) + \Gamma_t(S_{t-1}, S_t)\right] \quad (9)$$

with initial conditions: $B_N(S_t) = 0$ for $S_t = 0$ and $B_N(S_t) = -\infty$ for $S_t \neq 0$

For a non-terminated trellis, $B_N(S_t) = \log(1/2^m)$ for $S_t = 0$ and $B_N(S_t) = \log(1/2^m)$ for $S_t \neq 0$ with m being the overall encoder memory. For the log-MAP algorithm,

$$\max^{*}(a,b) = \max(a,b) + \log\left(1 + e^{-|a-b|}\right) \quad (10)$$

The omission of the correction function $\log\left(1+e^{-|a-b|}\right)$ results in the max-log-MAP algorithm where $\max^{*}(a,b) = \max(a,b)$. The expression for *LLR* becomes

$$LLR = \max_{R_1}^{*}\left[A(S_{t-1}) + \Gamma_t(S_{t-1}, S_t) + B(S_t)\right] - \max_{R_0}^{*}\left[A(S_{t-1}) + \Gamma_t(S_{t-1}, S_t) + B(S_t)\right] \quad (11)$$

R_1 and R_0 denote transitions associated with inputs +1 and -1 respectively.

III. Variable Rate Superorthogonal Turbo Code (VRSTC)

In [3], a technique was designed to maintain the orthogonality of the codewords in a Variable Rate Superorthogonal Convolutional (VRSC) code instead of puncturing a bit out of an OVSF codeword. In this work, this mechanism has been applied in a VRSTC system. Fig. 5 depicts a VRSTC encoder. The only difference between this encoder and the one in Fig. 3 is that puncturing block is introduced between the shift registers and the OVSF code tree block. The puncturing matrix used in this work is

$$P_M = \begin{bmatrix} 1 & 1 \\ 1 & 0 \\ 1 & 1 \end{bmatrix}$$

The VRSTC encoder operates almost in the same manner as the superorthogonal turbo encoder in Fig. 3. With the introduction of the puncturing block, the code becomes both variable and orthogonal. Regarding the VRSTC encoder in Fig. 5 with $K_c = 5$, excluding the first and last stages, the remaining bits in the shift registers enter the puncturing block at time $t = 0$. Considering the first column of P_M, no puncturing occurs and the bits move to the OVSF tree block where a codeword of length $n = 8$ bits is selected. At time $t = 1$, the second column of P_M indicates that the middle bit must be deleted (out of the next three remaining bits in the shift register), and the remaining two unpunctured bits select a codeword of length $n = 4$ in the OVSF tree block. At time $t = 2$, the first column of P_M is again selected resulting in no puncturing. In this way, codewords of variable lengths are obtained, and the orthogonality of the codewords is kept. The code rate of the upper encoder is $1/8$ and that of the lower encoder is ¼. Hence, the overall code rate of the VRSTC system is $1/12$.

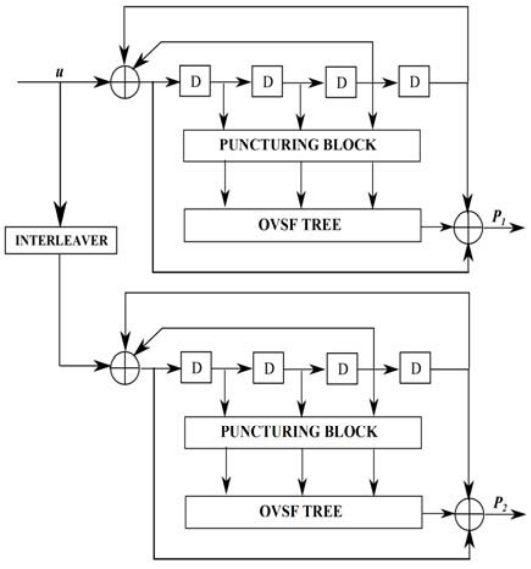

Fig. 5 VRSTC Encoder

Fig. 6 illustrates the VRSTC trellis. As the overall memory is $m = 4$, the trellis consists of 16 states. Input bits 0 and 1 are

associated with dotted and solid lines respectively. Branches corresponding to the "no puncturing case" are labeled with eight-bit codes (left hand side) whereas branches corresponding to the punctured case are marked with four-bit codes. The structure of the trellis is the same for unpunctured and punctured codewords, but only the size of the codeword changes. This scheme not only varies the rate but it also uses the same trellis for decoding while maintaining orthogonality between the codewords. The trellis structure is kept fixed to simplify the decoding process. The superorthogonal turbo encoder and the VRSTC encoder in Figs. 3 and 5 respectively are recursive encoders. Although it was mentioned in sub-Section II *B* that the systematic bits are not sent, the recursiveness of the encoders leads to a systematic code. In Fig. 6, it can be observed that the systematic bit is present in each codeword at the fifth underlined position for the unpunctured codewords. As for the punctured ones, the systematic bits are found in the third underlined position of each codeword.

IV. Performance Evaluation

Computer simulations were carried out to evaluate the performance of superorthogonal turbo codes employing OVSF codes with different numbers of blocklength in the AWGN channel. Results as bit error rate and block error rate curves are illustrated in Figs. 7 to 14 for N = 200, 1000, 4000 and 5400.

For all graphs, bit error rate curves gave better performance than the block error rate curves due to the fixed number of block errors used to stop the decoding. Constraint length K_c = 5 was used in the simulations and the feedback polynomial in the superorthogonal turbo code was 23 (octal). The overall code rate of the unpunctured and punctured codes were $^1/_{16}$ and $^1/_{12}$ respectively. Only the upper encoder was terminated while the other one was left open. Decoding was performed with the MAP, log-MAP and max-log-MAP algorithms with 16 iterations.

The results obtained for unpunctured codes were compared to [5] where Walsh-Hadamard codes were employed. In small blocklengths, such as N = 200, the bit error rate is slightly worse at E_bN_o = 0.5 and E_bN_o = 1.0, and slightly better at E_bN_o = 1.5 and E_bN_o = 2.0 in [5]. When compared with N =1000 bits in [5], there is a loss of 0.3 dB at a bit error rate of 10^{-3}. Despite the loss of performance, the superorthogonal turbo codes with the OVSF code have advantages of accommodating variable rate transmission while keeping the orthogonality of the codewords with the VRSTC system. With OVSF codes, different sequence lengths in the same tree can be obtained as opposed to a Walsh-Hadamard matrix described in Subsection II *A*.

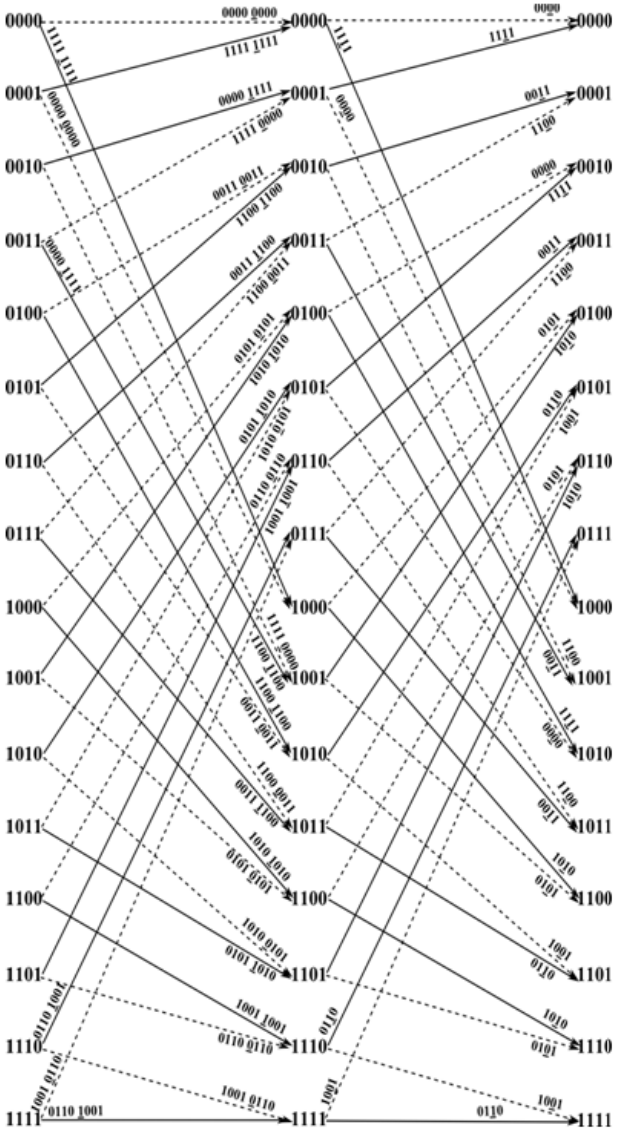

Fig. 6 VRSTC Trellis

Figs. 7 and 8 demonstrate bit error rate and block error rate results respectively, obtained with N = 200 bits with the MAP, log-MAP and max-log-MAP algorithms. The unpunctured codes for all algorithms give better performance than the punctured ones. The best performance is obtained with the log-MAP algorithm although eventually it gives the same performance as the MAP one. The max-log-MAP algorithm exhibits the worst performance (punctured max-log-MAP code) with the replacement of the term max^* with max. Hence, the omission of the correction term results in performance degradation. The benefit of log-MAP decoding over max-log-MAP decoding is that performance gains of 0.25dB and 0.2dB are obtained at bit error rate and block error rate of 10^{-3} respectively for unpunctured codes. For N = 1000 bits, performance gains of 0.27dB and 0.25dB (unpunctured codes) have been achieved in Figs. 9 and 10 respectively with the

log-MAP algorithm over the max-log-MAP one for error rates of 10^{-3}.

The advantage of using random interleaving is that the performance increases when N becomes larger. The reason behind is that a large interleaver has the tendency of bringing further apart the successive bits of the original data. When comparing bit error rate results of Figs. 11 and 12 for N = 4000 and N = 5400 respectively with previous graphs of smaller blocklengths, it can clearly be observed that better performance is obtained with all three decoding algorithms as N is increased. For N = 4000 bits, performance gains of 0.32dB and 0.31dB have been achieved in Figs. 11 and 12 respectively with the log-MAP algorithm over the max-log-MAP one for error rates of 10^{-1}. For N = 5400 bits, performance gains of 0.325dB and 0.30dB were reported in Figs. 13 and 14 respectively for the same error rates. In [5], the results were compared to an ordinary rate $^1/_3$ turbo code with generator polynomials of 23 and 35 (octal) where a performance advantage was observed. Unpunctured superorthogonal turbo codes with the OVSF code also demonstrate the same behavior when compared in [5], and this is achieved at the expense of bandwidth expansion resulting in appropriate variable rate applications in CDMA.

The time taken by the simulations for N = 4000 and N = 5400 were recorded and plotted in Fig. 15. They were achieved with Quad-Core processors on Ubuntu Operating System. Obviously, the punctured codes take less time than the unpunctured ones as bits have been deleted in the shift registers during the encoding process according to P_M. It is known that Log-MAP decoding minimizes computational complexity compared to MAP. It also exhibits almost the same performance than the MAP algorithm. As N is increased, better performance is observed. As simulations were stopped when a fixed number of block errors were obtained, the Log-MAP algorithm took the longest time to complete the simulations as there were more error-free blocks, and more time was required to achieve the required number of block errors, hence explaining the increase simulation time. The max-log-MAP algorithm takes the least decoding time, as it is simpler and faster to implement but at the expense of performance degradation. All punctured codes are also suitable for implementation as decoding takes less time despite the loss in performance. Moreover, variable rate is obtained with the orthogonality of the codewords being kept. The punctured version could find its use in real-time applications such as in Hybrid Automatic Repeat reQuest (HARQ) systems where forward error correction is utilized.

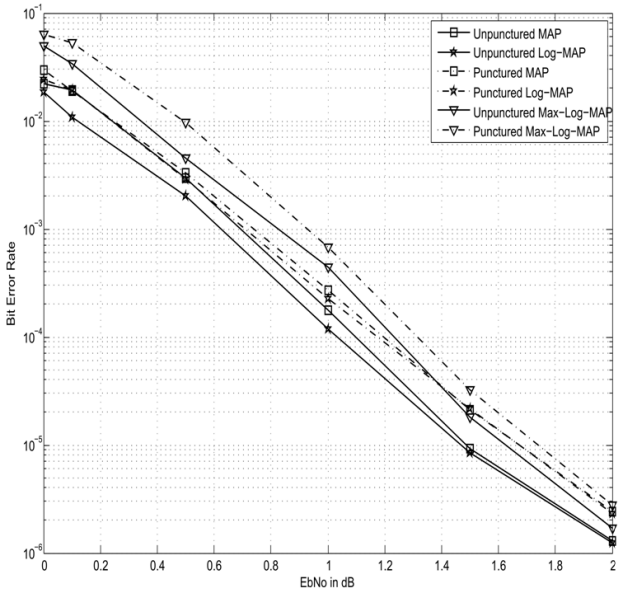

Fig. 7 Bit Error Rate Against E_bN_o N = 200 bits

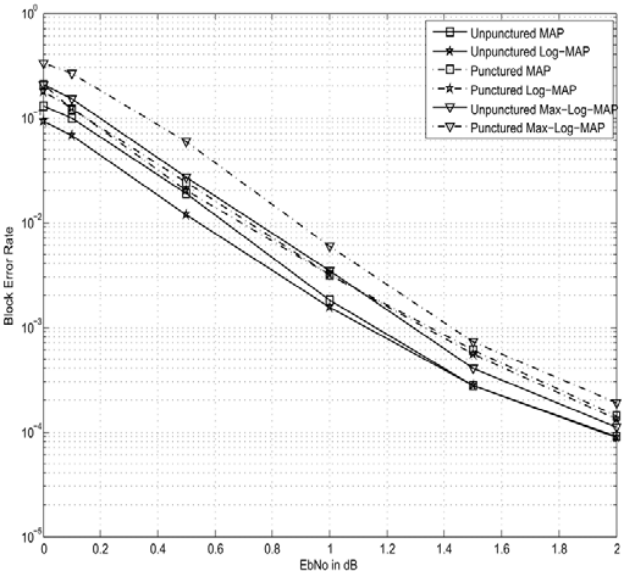

Fig. 8 Block Error Rate Against E_bN_o N = 200 bits

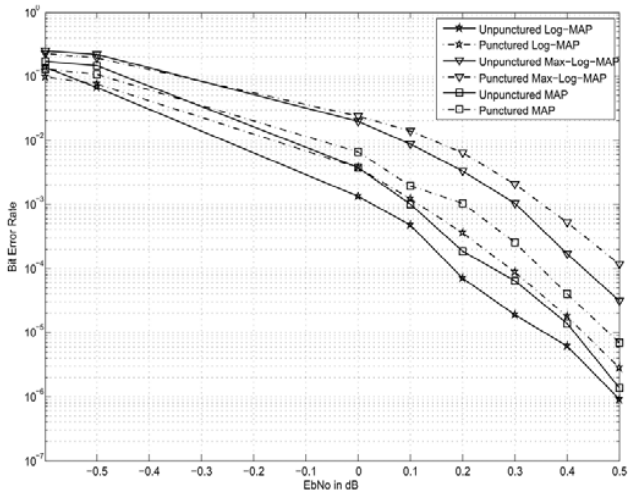

Fig. 9 Bit Error Rate Against E_bN_o N = 1000 bits

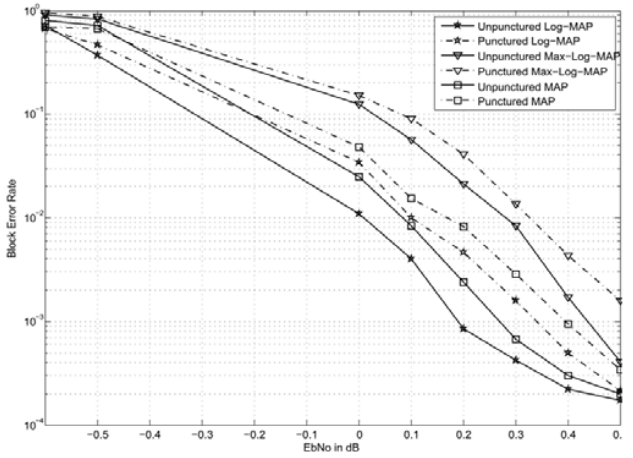

Fig. 10 Block Error Rate Against E_bN_o N = 1000 bits

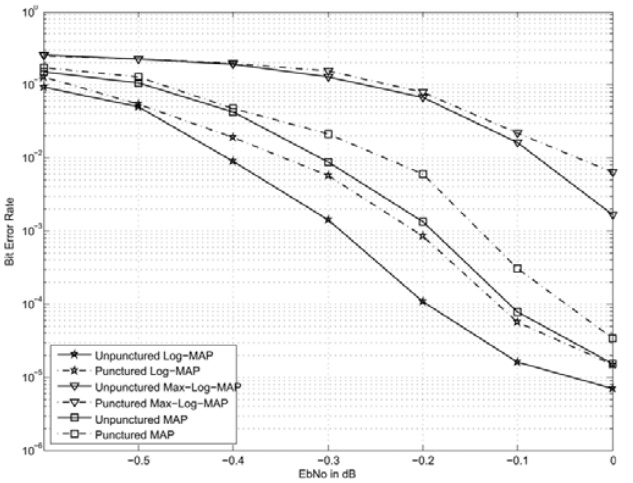

Fig. 11 Bit Error Rate Against E_bN_o N = 4000 bits

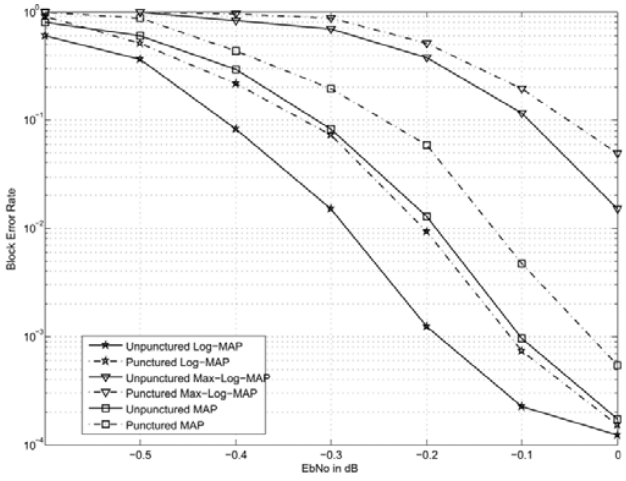

Fig. 12 Block Error Rate Against E_bN_o N = 4000 bits

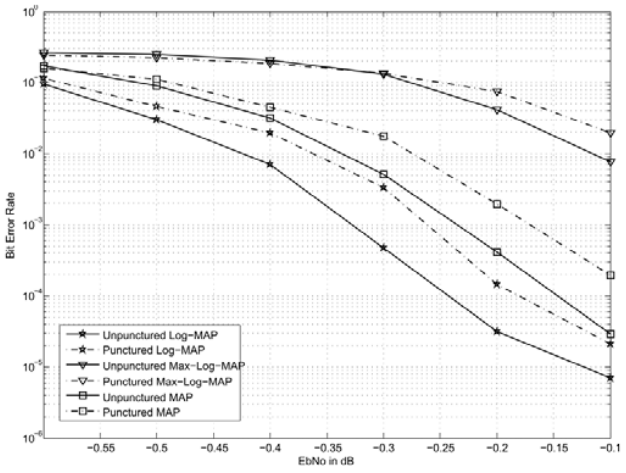

Fig. 13 Bit Error Rate Against E_bN_o N = 5400 bits

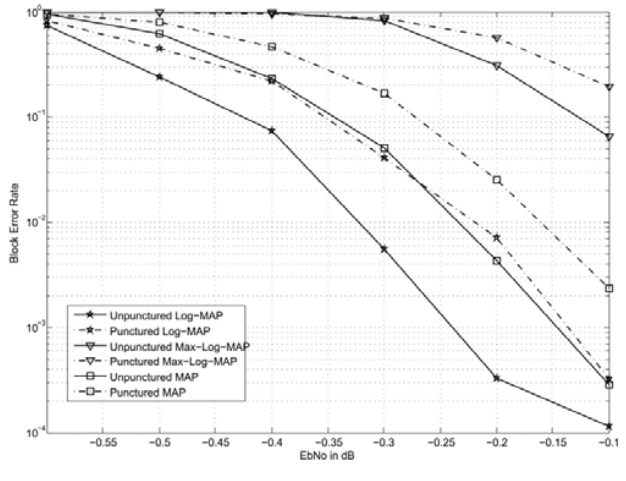

Fig. 14 Block Error Rate Against E_bN_o N = 5400 bits

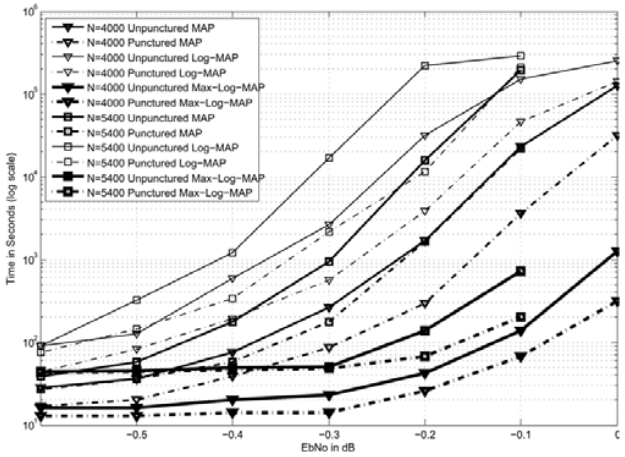

Fig. 15 Time (log scale) against E_bN_o for Unpunctured and Punctured Codes $N = 4000$ and $N = 5400$

V. Conclusion

It was seen how variable-rate in the VRSTC could be achieved in superorthogonal turbo coding with OVSF codes. Simulation results demonstrate better performance than higher rate (rate $^1/_3$) ordinary turbo codes at the expense of bandwidth expansion. Although, the MAP simulations results show decreased performance compared to those using Walsh-Hadamard codes, the utilization of OVSF codes have many advantages including the storage of a single OVSF tree to produce variable-length codewords compared to the storage to many matrices of various lengths to achieve the same for Walsh-Hadamard codes. Moreover, the orthogonality of codewords is kept with the VRSTC system. The decoding algorithms used show very good performance at lower E_bN_o with increasing blocklengths. The VRSTC scheme is thus suitable for use in CDMA and in future mobile communications systems to support many types of applications where variable-rate is a prerequisite.

Acknowledgment

The assistance and guidance of Dr. G. Ramsawock in this research work, and the financial support of the Tertiary Education Commission of Mauritius are gratefully acknowledged.

References

[1] C. Berrou, A. Glavieux, and P. Thitimajshima, "Near shannon limit error-correcting coding and decoding: Turbo-codes," *IEEE International Conference on Communications ICC'93*, Geneva, Switzerland 23-26 May 1993, vol. 2, pp. 1064-1070.

[2] B. Sklar, "Turbo code concepts made easy, or how I learned to concatenate and reiterate," *MILCOM 97*, vol. 1, pp. 20-26.

[3] G. Ramsawock, "Combined channel coding and modulation using variable rate," Ph.D. dissertation, University of Mauritius, Mauritius, 2009.

[4] A. Lientz and J. Villasenor, "Very low variable rate convolutional codes for unequal error protection in DS-CDMA systems," *IEEE Transactions on Communications*, July 1997, vol. 45, no. 7, pp. 753-755.

[5] K. Pehkonen and P. Komulainen, "A superorthogonal turbo-code for CDMA applications," *IEEE 4th International Symposium on Spread Spectrum Techniques and Applications Proceedings*, 22-25 Sep 1996, vol. 2, pp. 580-584.

[6] P. Komulainen and K. Pehkonen, "Performance evaluation of superorthogonal turbo codes in AWGN and flat rayleigh fading channels," *IEEE Journal on Selected Areas in Communications*, vol. 16, no. 2, 1998, pp. 196-205.

[7] A.J. Viterbi, "Method and apparatus for generating superorthogonal convolutional codes and the decoding thereof," US005193094A, March 9, 1993.

[8] A.J. Viterbi, *CDMA: Principles of Spread Spectrum Communication*. Addison-Wesley Publishing Company, ISBN 0-207-63374-4, 1995.

[9] L. Yen and M. Tsou, "An OVSF code assignment scheme utilizing multiple RAKE combiners for W-CDMA," *Computer Communications*, vol. 27, no.16, 2004, pp. 1617-1623.

[10] G. Suchitra and M.L. Valarmathi, "BER performance of modified walsh hadamard codes in a DS-CDMA and cognitive underlay system," *European Journal of Scientific Research*, vol. 64, no. 4, 2011, pp. 563-578.

[11] M.H. Le and R. Liyana-Pathirana, "Unequal error protection codes for wavelet image transmission over W-CDMA, AWGN and rayleigh fading channels," *10th International Conference on Telecommunications, ICT 2003*, 23 Feb - 1 March 2003, vol. 2, pp. 1140-1146.

[12] P. Robertson, "Illuminating the structure of code and decoder of parallel concatenated recursive systematic (turbo) codes," *IEEE Global Telecommunications Conference, GLOBECOM'94*, San Francisco, CA, 28 Nov- 2 Dec 1994, vol. 3, pp. 1298-1303.

[13] R. L. Bahl , J. Cocke , F. Jelinek and J. Raviv, "Optimal decoding of linear codes for minimizing symbol error rate," *IEEE Transactions on Information Theory*, vol. 20, no.2, 1974, pp. 284-287.

[14] P. Robertson, E. Villebrun and P. Hoeher, "A comparison of optimal and sub-optimal MAP decoding algorithms operating in the log domain," *Proceedings of the International Conference on Communications*, vol. 2, 1997, pp. 1009-1013.